View metadata, citation and similar papers at core.ac.uk

brought to you by CORE

provided by Calhoun, Institutional Archive of the Naval Postgraduate School

Calhoun: The NPS Institutional Archive

Faculty and Researcher Publications | Faculty and Researcher Publications Collection

2016-02

Using Shifting Masses to Reject Aerodynamic Perturbations and to Maintain a Stable Attitude in Very Low Earth Orbit

Virgili-Llop, Josep

http://hdl.handle.net/10945/50863

DUDLEY KNOX LIBRARY

http://www.nps.edu/library

Calhoun is a project of the Dudley Knox Library at NPS, furthering the precepts and goals of open government and government transparency. All information contained herein has been approved for release by the NPS Public Affairs Officer.

Dudley Knox Library / Naval Postgraduate School
411 Dyer Road / 1 University Circle
Monterey, California USA 93943

AAS 16-354

USING SHIFTING MASSES TO REJECT AERODYNAMIC PERTURBATIONS AND TO MAINTAIN A STABLE ATTITUDE IN VERY LOW EARTH ORBIT

Josep Virgili-Llop[*], Halis C. Polat[†] and Marcello Romano[‡]

The aerodynamic forces are the main orbital and attitude perturbations at very low orbital altitudes ($\lesssim$450 km). To minimize them, it is desirable to design spacecraft with their center-of-mass (CoM) as close as possible to the spacecraft's center-of-pressure (CoP). Design constraints, poorly understood aerodynamics and environment variability, prevent this CoP and CoM match. The use of internal shifting masses, actively changing the location of the spacecraft CoM, and thus modulating, in direction and in magnitude, the aerodynamic torques is proposed as a method to reject these disturbances. First, the equations of motion of a spacecraft with internal moving parts are revisited. The atmospheric environment and the aerodynamic properties of a spherically shaped spacecraft are then provided. A single-axis controller is used to analyze the disturbance rejection capability of the method with respect to several parameters (shifting mass, shifting range and altitude). This analysis shows that small masses and a limited shifting range suffice if the nominal CoM is relatively close to the estimated CoP. For the full three rotational degrees-of-freedom analysis, a quaternion feedback controller and a linear-quadratic regulator are used. Finally, a practical implementation on a 3U CubeSat using commercial-off-the-shelf components is provided, demonstrating the technological feasibility of the proposed method.

INTRODUCTION

Operating at lower altitudes can provide several benefits to Earth observation missions.[1,2] By lowering the operational altitude, the resolution of a given optical instrument, the radiometric performance of the sensor and the geospatial accuracy of the imagery are improved. For radar payloads, either the antenna size or the transmission power can be decreased. Furthermore, the launcher can usually deliver more payload at lower altitude orbits or, for a given spacecraft mass, a smaller and potentially more cost-effective launcher can be used. Although the orbital decay caused by aerodynamic drag is perceived as the main drawback of these very low altitude orbits, some studies suggest that the cost-effectiveness of the system can be increased by reducing the operational altitude.[3]

The presence of strong aerodynamic forces can also be an advantage. As the lifetime is reduced, there is no need to de-orbit spacecraft at their end-of-life. Space debris also decay at a faster rate, reducing the collision risk and greatly increasing the required object density to generate a Kessler syndrome runaway.[4] Furthermore, the aerodynamic forces can also be used for attitude and orbit control.[5–10]

[*]Postdoctoral Research Associate, Spacecraft Robotics Laboratory, Naval Postgraduate School, 700 Dyer Road, Monterey CA 93940, USA.

[†]Graduate Student, Spacecraft Robotics Laboratory, Naval Postgraduate School.

[‡]Associate Professor, Spacecraft Robotics Laboratory, Naval Postgraduate School.

Despite the aerodynamic forces potential use, for certain missions it may be desirable to minimize their perturbations. An effective and conceptually simple measure to lower the aerodynamic forces for a given operational altitude is to reduce the spacecraft's cross section area exposed to the incident flow. For this very reason, vehicles operating at very low altitudes tend to be slender.[11,12] To minimize the attitude perturbation it is also desirable to design spacecraft with their center-of-mass (CoM) as close as possible to the spacecraft's center-of-pressure (CoP), minimizing the force lever arm and reducing the disturbance torque. The CoP location is uncertain as spacecraft aerodynamics are not well understood[13,14] and due to environment variability.[15,16] Additional practical design constrains on the location of the CoM make the realization of an overlapping CoP and CoM impossible in practice.

The orbit range commonly known as Low Earth Orbit (LEO) is usually defined as those orbits whose mean altitude extends up to 2000 km.[17,18] As the aerodynamic forces are only dominant in the lower part of the LEO range the term Very Low Earth Orbits (VLEO) is used in this paper to make clear that the considered orbit range only extends up to $\sim$450 km in altitude.[1,2]

Attitude perturbations can be compensated for by using traditional attitude control actuators. At very low altitudes the aerodynamic disturbance magnitude can be significant and can present a secular component. In this paper, the use of a set of internal shifting masses, actively changing the location of the spacecraft CoM, and thus modulating, in direction and in magnitude, the aerodynamic torques is proposed as a method to stabilize a spacecraft.

This method is not proposed as a complete substitute to traditional actuators but rather as a complement. When the shifting masses reject the aerodynamic disturbances the use of other actuators is reduced, potentially delaying their saturation, and potentially saving power and mass.

The use of shifting masses as attitude control actuators has already been proposed in the past to help detumble spacecraft,[19,20] control the coning motion of a spinning spacecraft,[21–23] control the pitch and yaw of solar-sails[24–26] and, in general, to complement traditional attitude control actuators.[27–29]

Of particular interest is the work by Chesi[30] who proposes the use of aerodynamic drag to generate attitude control torques modulated in magnitude and direction by actively shifting a set of internal masses. As the aerodynamic torque is perpendicular to the aerodynamic force (i.e. to the relative flow vector), the system is under-actuated and it needs to be augmented by other actuators. Although that particular work, simplifies the dynamic effects of the shifting masses, ignores the variable nature of the Earth's atmosphere and assumes that the aerodynamic properties are known and constant, it shows the conceptual feasibility of using shifting masses to control the aerodynamic torques. In particular, it shows that by using a set of three shifting masses augmented by reaction wheels or magnetic torquers and using an adaptive non-linear feedback control law, a spacecraft can be slowly brought, from any initial attitude and angular velocity, to a desired attitude while minimizing the use of the reaction wheels or magnetic torquers.

The work presented in this paper builds upon the original concept by Chesi and proposes the use of shifting masses to reject the aerodynamic disturbances and stabilize the spacecraft's attitude, considering the variability and uncertainty of the atmosphere and of the aerodynamic properties. Furthermore, by exploiting the ability to control the aerodynamic torques, other disturbances, such as gravity-gradient, residual magnetic dipole, and solar radiation pressure can also be partially compensated helping further reduce the use of traditional actuators to keep the spacecraft stable.

To keep the analysis as general as possible, a spherically shaped spacecraft will be assumed.

Although it may seem that this is a simplistic case, a spheric shape can already be used to illustrate the uncertainty on the aerodynamic properties without dwelling into specific shapes.

This paper is organized as follows. First, the equations of motion of a spacecraft with internal moving parts are revisited.[19,31] The uncertain nature of the aerodynamic disturbance caused by a variable atmosphere and the uncertain aerodynamics is then presented. A one rotational degree-of-freedom reduced model with one shifting mass driven by a Proportional-Integral-Derivative controller (PID) is then introduced. The disturbance rejection capability of the system with respect to several parameters (shifting mass, shifting range and operating altitude) is explored, showing that small masses and limited shifting ranges suffice if the nominal CoM is relatively close to the estimated CoP. The yaw rotation axis is used for the reduced model as the primary effects of atmospheric co-rotation and wind are on this axis. A full three degrees-of-freedom case with two shifting masses driven by a quaternion feedback based controller moving along the pitch and yaw axes and augmented by an ideal actuator in roll is later examined. Finally, a practical implementation, only using Commercial-Off-The-Shelf (COTS) components, on a 3U CubeSat and using a Linear Quadratic Regulator (LQR) controller is presented. This demonstrates that it is technically feasible to implement such a control method in nanosatellites.

MASS AND INERTIA MODEL

The spacecraft hosting the shifting masses (host spacecraft) is assumed to be a homogeneous density sphere with a discrete fixed point mass. This discrete fixed mass allows to displace the CoM of the host spacecraft from the sphere's geometric center. A homogeneous density sphere mass is $M_S = \rho_S 4/3\pi R^3$ and its inertia $I_S = \rho_s 8/15\pi R^5$, with ρ_S denoting the sphere's density and R its radius. The discrete mass $M_P = \kappa M_S$ can be expressed as a mass fraction κ with respect to the sphere's mass M_s. The total mass of the host vehicle is then $M_0 = M_S\,(1+\kappa)$.

Let the host spacecraft's CoM define the origin of the spacecraft's body axes B_0 with the fixed point mass located along the roll axis $\hat{i}$ as depicted in Figure 1. If the distance between the point mass and the sphere's center is denoted by d_{M_P}, the combined inertia of the host vehicle I_0 can be computed using Eq. (1). If $d_{M_P} > 0$ the CoM will be located in the positive side of $\hat{i}$ and if $d_{M_P} < 0$ then the CoM will be in the negative side of $\hat{i}$.

$$I_0 = I_S + \frac{M_S\,(1+\kappa)}{\kappa} \begin{bmatrix} 0 & 0 & 0 \\ 0 & d_{M_P}^2 & 0 \\ 0 & 0 & d_{M_p}^2 \end{bmatrix} \tag{1}$$

Note that the host spacecraft is symmetric with respect to the roll axis $\hat{i}$ and thus the definition of the pitch $\hat{j}$ and yaw $\hat{k}$ axes is arbitrary. The goal of the control is then to align the body axes B_0 with the orbital frame.

To this host vehicle, whose mass and inertia properties are fixed, known and constant, a set of N internal shifting masses m_n is added, altering the mass, CoM location and inertia of the resulting combined system. The general arrangement of the system is shown in Figure 1. As the body reference frame is defined with respect to the CoM of the host spacecraft (excluding the shifting masses) the combined system's CoM (including the shifting masses) will not be located at the origin of the body reference frame B_0.

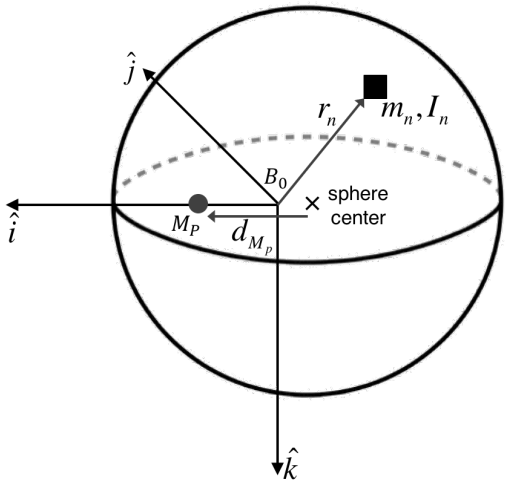

Figure 1. Schematics of the Spheric Spacecraft, with the Fixed Mass and the Shifting Masses .

DYNAMIC MODEL

The equations of motion for a system of connected rigid bodies will be used in order to take into account the dynamic effects of the shifting masses. This fundamental equation is given by Eq. (2).[19,31]

$$\tau = \dot{H} + S \times a \tag{2}$$

In Eq. (2) τ denotes the external torques applied at the reference point, $\dot{H}$ is the time derivative of the system's angular momentum, S is the system's first moment of mass with respect the reference point and a denotes the inertial acceleration of the reference point. This reference point is considered to be arbitrary and moving in an arbitrary manner. It is interesting to note that if the acceleration of the reference point is zero ($a = 0$) or if the reference point is selected as the system's CoM ($S = 0$) then the usual expression $\tau = \dot{H}$ is recovered.

Without loss of generality, the host vehicle CoM (origin of B_0) will be used as the reference point. This assumption is useful, as by definition, the host vehicle mass M_0 and inertia I_0 are constant in B_0 and as the movement of the shifting masses is known with respect to the host spacecraft.

The N shifting masses have their own reference frames B_n, with their origin in their own CoM and with arbitrary orientation. The inertia of the shifting masses in B_n will be denoted as $I_n^{B_n}$ and in B_0 will be denoted as simply I_n.

The location of B_n with respect to B_0 will be denoted as r_n. The $\dot{r}_n$ and $\ddot{r}_n$ terms will denote the inertial linear velocity and acceleration of the shifting mass in B_0 and ω_0 the angular velocity of the B_0. The inertial angular velocity of the shifting mass ω_n can be computed as in Eq. (3), with $\omega_n^{B_n}$ being the relative angular velocity of the shifting mass reference B_n with respect to the host vehicle reference B_0.

$$\omega_n = \omega_0 + \omega_n^{B_n} \tag{3}$$

In such a multiple body system, the total angular momentum H is composed of the sum of the host

vehicle and shifting masses angular momentum as shown in Eq. (4).

$$H = H_0 + \sum_{n=1}^{N} H_n \tag{4}$$

$$H_0 = I_0 \omega_0 \tag{5}$$

$$H_n = I_n \omega_n + m_n r_n \times \dot{r}_n \tag{6}$$

The linear inertial velocity of the shifting mass $\dot{r}_n$ can be simply computed using the following equation, with $\dot{r}'_n$ being the relative velocity of the shifting mass in B_0.

$$\dot{r}_n = \dot{r}'_n + \omega_0 \times r_n \tag{7}$$

To use Eq. (2) the angular momentum needs to be differentiated. Deriving Eq. (4) it follows that the total angular momentum time derivative is the sum of the host vehicle and shifting masses angular momentum time derivatives.

$$\dot{H} = \dot{H}_0 + \sum_{n=1}^{N} \dot{H}_n \tag{8}$$

$$\dot{H}_0 = I_0 \dot{\omega}_0 + \omega_0 \times H_0 \tag{9}$$

$$\dot{H}_n = I_n \dot{\omega}_n + \omega_n \times H_n + m_n r_n \times \ddot{r}_n \tag{10}$$

$$\dot{\omega}_n = \dot{\omega}_0 + \dot{\omega}_n^{B_n} \tag{11}$$

The inertial acceleration of the shifting masses can be written as follows.

$$\ddot{r}_n = \omega_0 \times (\omega_0 \times r_n) + \dot{\omega}_0 \times r_n + 2\omega_0 \times \dot{r}'_n + \ddot{r}'_n \tag{12}$$

Note how $\dot{r}'_n$ and $\ddot{r}'_n$ are the relative velocities and accelerations of shifting masses and thus can be measured and known. The first moment of mass is then defined as follows.

$$S = \sum_{n=1}^{N} m_n r_n \tag{13}$$

The inertial acceleration of the reference point (origin of B_0) can then be written as follows.

$$a = \ddot{r}_0 = \ddot{r}_c - \ddot{r} \tag{14}$$

The $\ddot{r}$ term denotes the acceleration of the system's CoM with respect to B_0 (the relative movement of the system's CoM) and $\ddot{r}_c$ is the inertial acceleration of the system's CoM (due to the external forces F). This $\ddot{r}_c$ acceleration can be easily computed using Newton's second law and $\ddot{r}$ is obtained by computing the relative CoM acceleration.

$$\ddot{r}_c = \frac{F}{M + \sum_{n=1}^{N} m_n} \tag{15}$$

$$\ddot{r} = \frac{\sum_{n=1}^{N} m_n \ddot{r}_n}{M + \sum_{n=1}^{N} m} \tag{16}$$

With the equations above, Eq. (2) can be expanded as in Eq. (17).

$$I_0\dot{\omega}_0 + \omega_0 \times I_0\omega_0 + \sum_{n=1}^{N} I_n\dot{\omega}_n + \sum_{n=1}^{N} \omega_n \times (I_n\omega_n + m_n r_n \times \dot{r}_n) + \sum_{n=1}^{N} (m_n r_n \times \ddot{r}_n) + ...$$
$$... + \frac{1}{M + \sum_{n=1}^{N} m_n} \left(\sum_{n=1}^{N} m_n \ddot{r}_n \right) \times \sum_{n=1}^{N} m_n r_n = \tau + \frac{F}{M + \sum_{n=1}^{N} m_n} \times \sum_{n=1}^{N} m_n r_n \quad (17)$$

The aerodynamic effects on the attitude dynamics of the system are represented by the external torques τ and forces F. Note that the torques τ are applied at the reference point (the host vehicle CoM) and not with respect to the system's CoM. The term in Eq. (17) that contains the external forces F accommodates this difference.

Point mass simplification

A useful simplification is obtained when it is assumed that the shifting masses are point masses and do not have inertia $I_n = 0$. Under this assumption, the general equations of motion (Eq. (17)) can be simplified as in Eq. (18).

$$I_0\dot{\omega}_0 + \omega_0 \times I_0\omega_0 + \sum_{n=1}^{N} (m_n r_n \times \ddot{r}_n) + \frac{1}{M + \sum_{n=1}^{N} m_n} \left(\sum_{n=1}^{N} m_n \ddot{r}_n \right) \times \sum_{n=1}^{N} m_n r_n = ...$$
$$... = \tau + \frac{F}{M + \sum_{n=1}^{N} m_n} \times \sum_{n=1}^{N} m_n r_n \quad (18)$$

For a single point mass and introducing the concept of reduced mass μ as in Eq. (19), the equation can be further simplified to finally obtain Eq. (20) and thus recover the expression from Edwards.[19]

$$\mu = \frac{mM}{M + m} \quad (19)$$

$$I_0\dot{\omega}_0 + \omega_0 \times I_0\omega_0 + \mu r_m \times \ddot{r}_m = \tau + \frac{\mu F}{M} \times r_m \quad (20)$$

AERODYNAMIC MODELING

The residual atmosphere present at orbital altitudes cause aerodynamic forces. Orbital decay is the main effect of aerodynamic drag but these aerodynamic forces will also induce aerodynamic torques and thus perturb the spacecraft's attitude.

In general, Eqs. (21)-(22) are used to compute aerodynamic forces, with ρ denoting the atmospheric density, V the relative velocity of the spacecraft with respect to the flow, A_{ref} an arbitrary reference area (usually taken as the cross section), and C_D and C_L the drag (anti-velocity) and lift (normal to velocity) coefficients respectively.

$$D = \frac{1}{2}\rho V^2 A_{ref} C_D \quad (21)$$

$$L = \frac{1}{2}\rho V^2 A_{ref} C_L \quad (22)$$

The atmospheric density ρ, the relative velocity with respect to the flow V and the force coefficients C_D and C_L need to be estimated before the aerodynamic forces can be computed. Unfortunately, the atmospheric environment is very variable and poorly predictable[15,16] and spacecraft aerodynamics are not particularly well understood.[13,14]

Realistic atmospheric and spacecraft aerodynamic models will be used to obtain what will be assumed as the truth values. The controller will then estimate these magnitudes using simplified aerodynamics and atmospheric models. This arrangement ensures the presence of realistic atmospheric variability and realistic aerodynamic properties, while emulating the uncertainty that the controller will be subjected to.

Atmospheric Density Model

The NRLMSISE-00[32] atmospheric model will be used to estimate the atmospheric density ρ. This specific atmospheric model offers a good balance between model accuracy and computational complexity.[33]

The Earth's atmosphere not only exhibits vertical density variations but also horizontal variability (e.g. the day-to-night density changes). Figure 2 shows the variation from the mean density for a 10:30 Local Time of Ascending Node (LTAN) circular Sun-synchronous orbit at different orbit altitudes in moderate solar activity.[34] Figure 2 exemplifies how variable the density and by extension the aerodynamic forces and torques are.

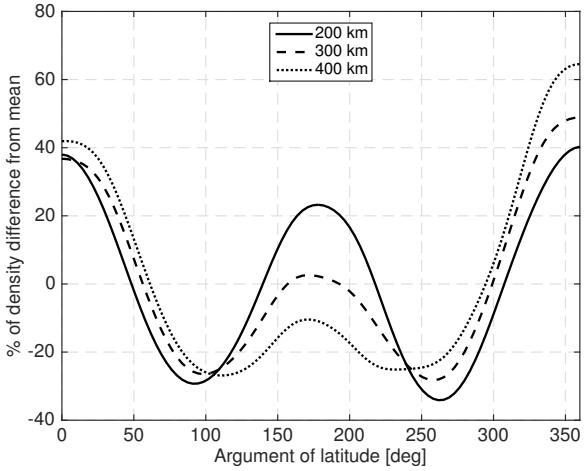

Figure 2. Density Variations During a Circular Sun-Synchronous Orbit at Different Operational Altitudes.

Wind Model

The atmosphere co-rotates with the Earth[35–37] and there is atmospheric time-varying wind.[38,39] These two effects will make the direction and magnitude of the relative flow V differ, in direction and in magnitude, from the inertial velocity.

The atmospheric wind is also highly variable, spatially and temporally. Figure 3a shows an example distribution of the wind according to the HWM93[40] model at 450 km with moderate solar activity[34] during northern hemisphere summer solstice. As the atmospheric wind has not been as extensively studied as other atmospheric properties, the existing models are less accurate[15] and

so the HWM07[41] state-of-the-art wind model will be used. It has to be noted that this model only provides zonal and meridional wind profiles representative of the climatological averages for various geophysical conditions. Vertical winds, which usually have smaller magnitudes, are not included in the model.

Figure 3b shows the sideslip angle caused by the atmospheric co-rotation and wind (using the HWM07 model) assuming that a spacecraft is pointed along the inertial velocity in a 10:30 LTAN circular Sun-synchronous orbit at different altitudes in moderate solar activity.[34]

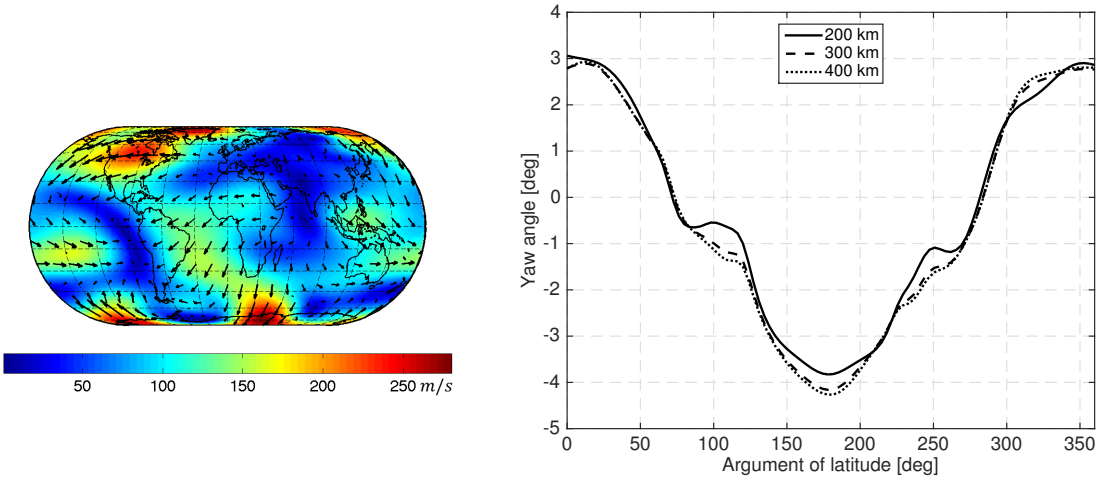

(a) (b)

Figure 3. Wind Pattern and Sideslip Angle.

Gas-Surface Interaction Model

In the orbital environment (>200 km in altitude) the residual atmosphere can no longer be considered as a continuum but needs to be considered as a rarefied-gas due to its low density.[42] For typical spacecraft sizes, the mean free path of a gas particle is much greater than a representative spacecraft dimension.[2] Consequently, it can be assumed that the interactions between gas particles (collisions) are very rare, and thus they can be safely ignored. The Gas-Surface Interactions (GSI) completely dominate the interaction of the spacecraft with the surrounding gas.

There are several GSI models[42] and here the Sentman model[43] will be used as it is the *de facto* standard to compute spacecraft aerodynamic coefficients at low orbital altitudes.[13,44] A comprehensive description of the models used in spacecraft aerodynamics can be found in other references.[13,14]

The Sentman model takes into account the thermal velocity distribution of the gas particles and assumes that all the incident gas particles that collide with a surface are adsorbed to be later diffusely reemitted. In the LEO range this seems to be true from the limited available orbital data.[45,46] The particles are reemitted with partial thermal equilibrium with the spacecraft surface. The degree of thermal equilibrium is denoted by the energy accommodation coefficient σ_a. In this model, the C_d and C_l can be written, following Sutton notation,[47] as in Eqs. (23) and (24).

$$C_D = \frac{\int C_d dA}{A_{ref}} \quad C_d = \left[\frac{P}{\sqrt{\pi}} + \gamma Q Z + \frac{\gamma}{2} \frac{v_r}{v_\infty} \left(\gamma \sqrt{\pi} Z + P \right) \right] \tag{23}$$

$$C_L = \frac{\int C_l dA}{A_{ref}} \quad C_l = \left[lGZ + \frac{l}{2}\frac{v_r}{v_\infty}\left(\gamma\sqrt{\pi}Z + P\right)\right]\frac{dA}{A_{ref}} \tag{24}$$

$$\gamma = \cos(\varphi) \quad l = \sin(\varphi) \tag{25}$$

$$G = \frac{1}{s_\infty^2} \quad P = \frac{1}{s_\infty} e^{-\gamma^2 s_\infty^2} \tag{26}$$

$$Q = 1 + G \quad Z = 1 + erf(\gamma s_\infty) \tag{27}$$

The φ term denotes the angle between the flow and the local normal vector (0 deg when the surface is normal to the flow and 90 deg when it is parallel), v_r the most probable velocity of the reemitted gas particles, v_∞ the relative bulk velocity between the spacecraft and the incident gas particles, and s is the ratio between v_∞ and the thermal velocity of the gas v_{th} ($s = \frac{v_\infty}{v_{\text{th}}}$).

According to Koppenwallner[48] the v_r/v_∞ ratio can be written as in Eq. (28) with R_g denoting the gas constant and T_w the temperature of the surface (wall).

$$\frac{v_r}{v_\infty} = \sqrt{\frac{1}{2}\left[1 + \sigma_a\left(\frac{4R_g T_w}{v_\infty^2} - 1\right)\right]} \tag{28}$$

From the limited orbital data available the energy accommodation coefficient is between 0.8 and 1.[44] The spacecraft surface temperature will be assumed constant at $T_w = 300\,\text{K}$.

Note that the drag and lift coefficients are dependent on the atmospheric parameters. As the atmosphere has temporal and spatial variability the force coefficients will be variable during an orbit. These changes in the force coefficients are small and can be safely ignored given that the perturbations included in the environment models (e.g. changes in atmospheric density) are orders of magnitude larger. Although, the Sentman model can provide the lift coefficient C_L it is, in general, an order of magnitude smaller than the drag coefficient C_D and thus it will be neglected in this analysis.[49]

Aerodynamic Properties of a Sphere

Due to the sphere symmetry, the drag coefficient is constant regardless of the orientation of the sphere with respect to the flow. Figure 4 shows the drag coefficient of a sphere (with $A_{\text{ref}} = \pi R^2$), clearly showing how the drag coefficient changes with altitude, solar activity and energy accommodation coefficient.

The usual body reference frame with Euler angles roll ϕ, pitch θ and yaw ψ will be adopted. When roll, pitch and yaw are zero the body frame is aligned with the orbit frame, which has $\hat{k}$ pointing nadir, $\hat{i}$ along the inertial velocity vector and $\hat{j}$ completing the right hand triad. The relative flow direction will be defined with its own reference frame where the flow direction will be in the $-\hat{i}_{\text{flow}}$ axis. The orientation of this flow reference frame will be denoted by a flow pitch θ_{flow} and flow yaw ψ_{flow}.

Let R_{OB} denote the rotation matrix from the body to the orbital frame and R_{OF} the rotation matrix from flow to orbital frame. Therefore, $R_{BF} = R_{OB}^T R_{OF}$ is the rotation from the flow to the body reference frame. With these definitions the aerodynamic force in body axes can be written as in Eq. (29), with D denoting the aerodynamic drag.

$$F_{\text{aero}} = R_{BF}\begin{bmatrix} -D \\ 0 \\ 0 \end{bmatrix} \tag{29}$$

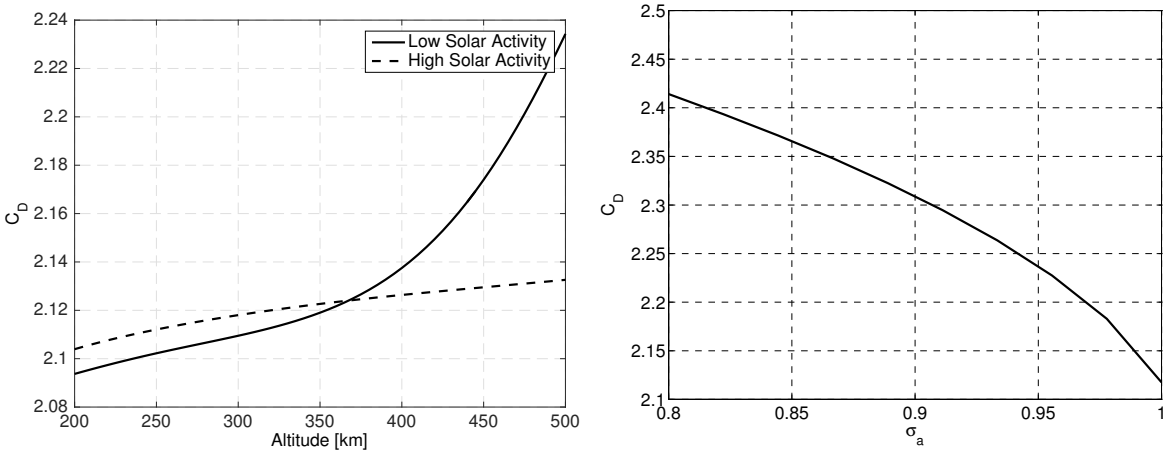

(a) (b)

Figure 4. Variation of a Sphere Drag Coefficient with Altitude, Solar Activity (a) and Energy Accommodation Coefficient (b).

The CoP of the sphere is aligned with the direction of the flow $\hat{i}_{\text{flow}}$ and its location along this axis can be computed using Eq. (30).

$$\frac{d_{\text{CoP}}}{R} = \frac{\int C_d(\varphi)\, x dA}{\pi R^2 C_D} = \frac{\int_0^{\pi}\int_0^{2\pi} C_d(\theta_{sc}, \phi_{sc}) \sin^2\phi_{sc} \cos\theta_{sc} d\theta_{sc} d\phi_{sc}}{\pi C_D} \approx 0.66 \tag{30}$$

Let $d_c = \kappa d_{M_P} / (1+\kappa)$ denote the distance between the center of the sphere and the origin of the body frame. The location of the spacecraft CoP in body axes can then be written as in Eq. (31).

$$p_{CoP} = \begin{bmatrix} -\mathrm{d_c} \\ 0 \\ 0 \end{bmatrix} + R_{BF} \begin{bmatrix} \mathrm{d_{CoP}} \\ 0 \\ 0 \end{bmatrix} \tag{31}$$

As the relative flow, the CoP and the center of the sphere, are aligned there is no torque with respect to the center of the sphere. The aerodynamic torque with respect the host vehicle CoM is then only a function p_{CoP} as shown in Eq. (32). It can then be assumed that torque-wise, the effective CoP is located at the center of the sphere.

$$\tau_{aero} = p_{CoP} \times F_{aero} = \begin{bmatrix} -\mathrm{d_c} \\ 0 \\ 0 \end{bmatrix} \times F_{aero} \tag{32}$$

It is useful to simplify these aerodynamic torque equations when the spacecraft is in close vicinity of its target attitude $\phi \approx 0$, $\theta \approx 0$, $\psi \approx 0$. As the atmospheric co-rotation and wind do not cause the relative flow to have large deviations with respect to the inertial velocities the θ_{flow} and ψ_{flow} magnitudes are also small. Under these assumptions, the Euler angles of the spacecraft with respect to the flow (rotation represented by R_{BF}) can be approximated using $\phi' = -\phi$, $\theta' = \theta_{\text{flow}} - \theta$ and $\psi' = \psi_{\text{flow}} - \psi$ (which will also be small angles) and the aerodynamic forces in body axes can be subsequently approximated by Eq. (33).

$$F_{aero} \approx -D \begin{bmatrix} \cos(\theta_{flow} - \theta)\cos(\psi_{flow} - \psi) \\ \cos(\theta_{flow} - \theta)\sin(\psi_{flow} - \psi) \\ -\sin(\theta_{flow} - \theta)\cos(\psi_{flow} - \psi) \end{bmatrix} \approx D \begin{bmatrix} -1 \\ -\psi' \\ \theta' \end{bmatrix} \tag{33}$$

A simplified expression for the aerodynamic torque can also be obtained using the same small angle approximation as shown in Eq. (34).

$$\tau_{aero} \approx D \begin{bmatrix} 0 \\ \theta' d_c \\ \psi' d_c \end{bmatrix} \tag{34}$$

From Eq. (34) it can be clearly seen that the equilibrium attitude is that attitude where the flow, host vehicle CoM and the sphere center are aligned ($\theta' = \psi' = 0$). When there is a misalignment of this equilibrium attitude, the aerodynamic torques will provide a restoring torque if the sphere center is behind the host vehicle CoM $d_{M_p} > 0$, making the spacecraft oscillate around this equilibrium point (marginally stable). If the host vehicle CoM is leading the center of the sphere $d_{M_p} < 0$ the system becomes unstable.

It is important to note that by definition the host vehicle CoM is displaced with respect to the sphere center only along the $\hat{i}$ direction. In a generic case, the CoM can be displaced in any direction and then a secular aerodynamic torque will appear when the spacecraft is at the target attitude (ignoring the variability of the relative flow direction). It is then desirable to have the CoM and effective CoP (center of the sphere) aligned with the $\hat{i}$ axis in order to avoid these secular torques.

As it is expected that spacecraft operating in VLEO take this issue into consideration it has been assumed that the CoM and CoP for the target stable attitude are reasonably aligned. Any residual misalignment can be corrected by a bias in the position of the shifting masses (resulting in a reduction of their shifting range and control authority).

Table 1. Numerical Parameters.

Parameter	Value
κ	0.1
ρ_s	$500\,\mathrm{kg\,m^3}$
C_D	2.2
σ_{C_D}	0.22 (10 % of the nominal $C_D = 2.2$)
Solar activity indices	Moderate activity as in[34]

REDUCED MODEL WITH ONE ROTATIONAL DEGREE-OF-FREEDOM

It is worth to start the analysis with a reduced model that only considers one rotational degree-of-freedom. This analysis will provide insight into the rejection capabilities and the shifting mass requirements with respect to the system parameters. It is also of particular interest to explore how the operating altitude drive the required shifting mass and range in order to meet pre-specified performance requirements. The yaw ψ rotation has been selected for this one-dimensional analysis as the co-rotation and predominant wind act on this particular axis. Additionally, a single shifting point mass will be used and the controller will be based on a reduced dynamic model (i.e. linearized). The goal of the shifting mass is then to stabilize the spacecraft around $\psi = 0$ and reject the disturbance induced by ψ_{flow}.

Under these assumptions, the equation of motion in Eq. (20) can be further simplified as in Eq. (35). The position, velocity and acceleration of the unique shifting mass with respect to the body axes is denoted by x, y and their time derivatives by $\dot{x}, \dot{y}$.

$$\left[I_z + \mu\left(x^2 + y^2\right)\right]\ddot{\psi} + \mu\left[2\left(x\dot{x}' + y\dot{y}'\right)\dot{\psi} + x\ddot{y}' - y\ddot{x}'\right] = \tau_z + \frac{\mu}{M}\left[F_x y - F_y x\right] \tag{35}$$

The aerodynamic disturbances have low frequencies (similar to the orbit frequency) and so it is expected the shifting masses motion will be also slow (small velocities and accelerations). Additionally, as the shifting mass m is small compared to the host vehicle mass $\mu \ll 0$, the dynamic effects of the shifting mass motion can be safely neglected.

As the shifting range is also small the change on the system's inertia is also small and thus it will be considered as constant (using the initial shifting masses position x_0 and y_0). These assumptions further simplify the equations of motion to Eq. (36). It also has to be noted that only the aerodynamic forces and torques will be considered.

$$\left[I_z + \mu\left(x_0^2 + y_0^2\right)\right]\ddot{\psi} = \tau_z + \frac{\mu}{M}\left[F_x y - F_y x\right] \tag{36}$$

Using the aerodynamic properties of a sphere and using the small angles approximation, Eq. (37) can be obtained.

$$\left[I_z + \mu\left(x_0^2 + y_0^2\right)\right]\ddot{\psi} = D\left(\psi' d_c + \frac{\mu}{M}\left[-y + \psi' x\right]\right) \tag{37}$$

It is immediately clear from Eq. (37) that to generate a control torque it is much more effective for the mass to move perpendicular to the relative flow (in this case y) than parallel to it (along x). So in order to limit the system complexity, it will be assumed that the shifting mass only moves in y (perpendicular to the flow if ψ' is small). Shifting the mass only along one direction reduces the volume and the complexity of the shifting mass system. It is understood that Eq. (37) has been simplified for small angles and thus shifting the mass along y will be perpendicular to the flow direction only for $\psi = \psi_{flow} = 0$. If there is a large misalignment the y shifting mass will start to loose efficacy.

Another important consideration that it is apparent from Eq. (37) is that the maximum torque provided by the shifting mass is $\tau_{max} = \pm D\frac{m}{M+m}y_{max}$. It is clear that the mass of the shifting mass and the available shifting range are the two parameters at the designer disposal.

The atmospheric density and the magnitude and direction of the flow are inherently unknown and thus an estimate of the density (based on the altitude) will be used and the incident flow will be assumed to match the inertial velocity magnitude and direction. Under these conditions the system equations can be written as Eq. (38), which corresponds to the transfer function written in Eq. (39). This represents a simple second order Single Input Single Output system and a Proportional-Integral-Derivative (PID) controller can be easily designed and implemented to reject the aerodynamic disturbances while keeping the spacecraft stable at $\psi = 0$.

$$\left[I_z + \mu\left(x_0^2 + y_0^2\right)\right]\ddot{\psi} = D\left(-\psi\left[\frac{\mu}{M}x_0 + d_c\right] - \frac{\mu}{M}y\right) \tag{38}$$

$$T(s) = \frac{\psi(s)}{y(s)} = \frac{b}{I's^2 + k} \tag{39}$$

$$I' = I_z + \mu\left(x_0^2 + y_0^2\right) \tag{40}$$

$$k = D\left(\frac{\mu}{M}x_0 + d_c\right) \tag{41}$$

$$b = -D\frac{\mu}{M} \tag{42}$$

To explore the design space and the system response it will be assumed that the PID controller is tuned so that the closed-loop system has a specific bandwidth and phase margin. In these fixed controller conditions a Monte Carlo analysis can be performed to extract the required shifting mass range for a given spacecraft size, aerodynamic properties and environmental conditions. Although the controller is build upon a linearized model, the numerical simulations use the full dynamic equations and the high-fidelity environment models. Additionally, the actual drag coefficient used in the numerical simulation differ from the one used to design the controller (emulating the uncertainty on the aerodynamic properties). Although the CoP is considered known, given that a spherical shape is used, the uncertainty on the drag coefficient can also be used to emulate an uncertainty in the CoP location. Sun-synchronous circular orbits with 10:30 am LTAN have been used.

The Monte Carlo simulations are initialized with ideal stable attitudes $\psi_0 = 0$ and $\dot{\psi} = 0$ and thus emulate steady state conditions. Each Monte Carlo run simulates 4 consecutive orbits and 100 simulations are used to extract the statistics (with error bars denoting the 95% confidence interval). The values shown in Table (1) are used for the simulations.

Figure 5 shows the maximum shifting range and attitude error (3σ values) for a 10 cm radius spherical satellite for different mass fractions of the shifting mass m/M and for a CoM leading the CoP by 3% of the sphere radius. Figure 6 shows how the required shifting range and attitude error change for different CoM to CoP distances d_p and with a fixed shifting mass fraction kept at 3% of the host vehicle mass M.

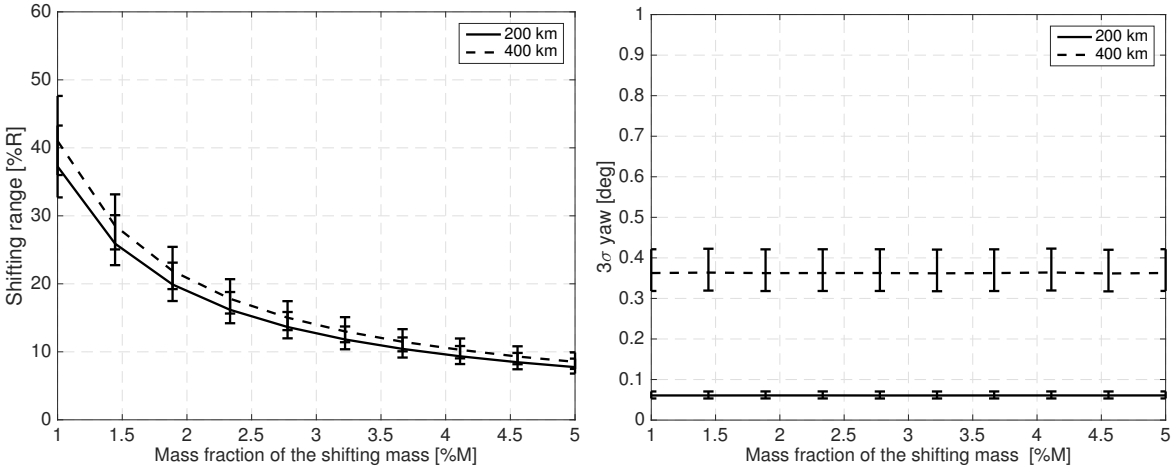

(a) (b)

Figure 5. Shifting Range (a) and Attitude Error (b) for Different Mass Fractions.

The system bandwidth in the controllers used to generate Figures 5 and 6 has been kept at four times the natural frequency of the system $4\omega_n$ and the phase margin has been set to 30 deg. This allows a comparison of the system performance even if the altitude is changed.

For a 10 cm radius case it is quite clear that the proposed method is able to reject the aerodynamic disturbances and maintain a reasonably stable attitude (even for unstable configurations) with mass

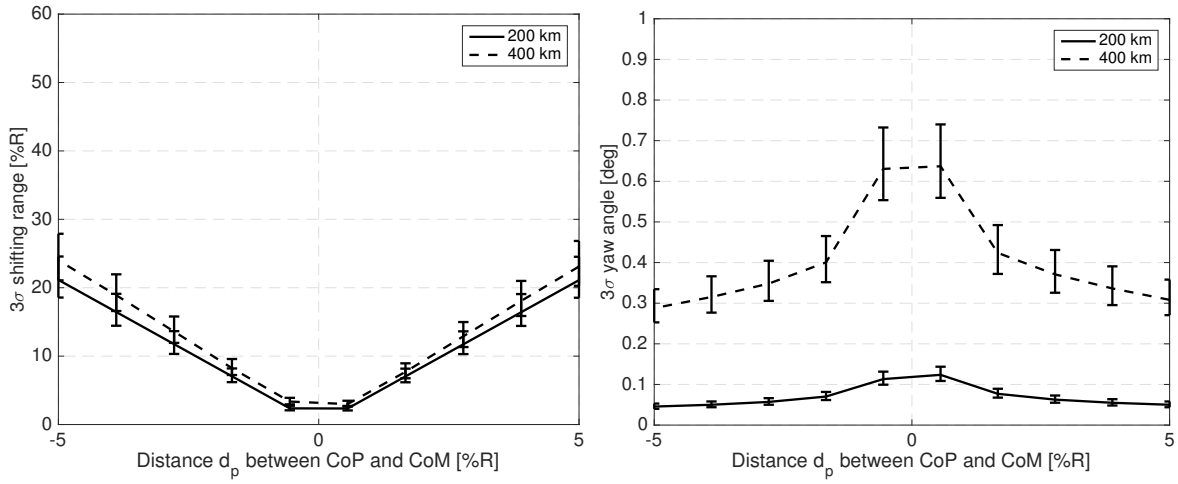

(a) (b)

Figure 6. Shifting Range (a) and Attitude Error (b) for Different CoP to CoM Distances.

fractions and shifting ranges requirements compatible with the spacecraft mass and dimension constrains. As expected the required mass fraction and required shifting range decrease as the CoP gets closer to the CoM. Also, unstable configuration $d_p < 0$ requires higher shifting range than their stable counterparts.

The attitude error, which is constant in Figure 5 due to the constant bandwidth employed, can be decreased if the bandwidth of the close-loop system is increased. The required shifting range can be decreased by decreasing the phase margin. Both measures have practical limits. By decreasing the phase margin the controller is less robust and increasing the bandwidth increases the gains which imposes more strict requirements on the sensors and actuators. It is also interesting to note that the relative shifting range increases slightly with altitude as a relative larger shifting is required to generate the same acceleration at higher altitudes where there atmosphere is less dense.

The tuning employed in this examples appears to give satisfactory results with the selected parameters and uncertainties. These examples illustrate the general trends and provide performance estimates that can be later used as initial guesses.

THREE ROTATIONAL DEGREES-OF-FREEDOM CASE

The previous analysis has been conducted using a reduced model and only considering a single rotational degree-of-freedom. That analysis is useful as provides generic results and shows the trends when the different parameters are varied. In this section a simple controller for the three rotational degree-of-freedom case will be presented.

Shifting mass driver

All the proposed control laws for the shifting masses specify their position and thus a driver that moves the shifting masses towards that location is required. A driver using a simple PID controller with the acceleration and shifting mass velocity limited to $R/10\,\mathrm{m/s^2}$ and $R\,m/s$ respectively has been employed.

Limiting the velocity and acceleration is particularly important when there are abrupt changes of the shifting masses position or velocity (i.e. during saturation), which could lead to significant dynamic effects that have been neglected during the controller design.

It has to be noted that although in this analysis the acceleration and velocity limits are tight to the sphere radius, smaller spacecraft, with proportionally less inertia, are more sensitive to the shifting masses internal movement and thus smaller limits may be required.

Quaternion feedback with partial feedback linearization

A more general approach that does not rely on linearization uses the well known quaternion feedback with partial feedback linearization.[50,51] The estimated aerodynamic torque $\hat{\tau}_{\text{aero}}$ is used to help with the feedback linearization but the terms related the shifting masses motion are left out as they are assumed to be negligible. Under this control law the requested torque can be written as in Eq. (43).

$$T_{\text{req}} = -k_p I q_e - k_d I \omega_{\text{req}} + \omega_0 \times I\omega_0 - \hat{\tau}_{\text{aero}} \tag{43}$$

In Eq. (43) q_e denotes the vector elements of the error quaternion,[50,51] ω_{req} denotes the target angular velocity (for a stable attitude with respect to the orbit frame it only includes a pitch rate that matches the orbital motion), I the inertia matrix and the k_p and k_d scalars denote the proportional and derivative gains respectively.

Some guidance to select the gains can be obtained by considering small angles, a single degree-of-freedom and that the shifting mass motion dynamics effects are negligible. In that case, the system reduces to a second order system and thus the proportional k_p and derivative gains k_d can be related to the closed-loop natural frequency ω_{cl} and damping ratio ξ as Eq. (44).[51]

$$k_p = 2\omega_{\text{cl}}^2 \quad k_d = 2\xi\omega \tag{44}$$

The quaternion feedback is particularly suited when large attitude misalignments are present and thus is will be employed here for a detumbling scenario. If it is assumed that the system is composed by three shifting masses each moving along the roll $\hat{i}$, pitch $\hat{j}$ and yaw $\hat{k}$, the aerodynamic torque provided by the shifting masses can be be written as follows (see Eq. (18)).

$$\tau_{\text{sm}} = \frac{F_{\text{aero}}}{M + m_1 + m_2 + m_3} \times \begin{bmatrix} m_1 r_1 \\ m_2 r_2 \\ m_3 r_3 \end{bmatrix} \tag{45}$$

With m_1, m_2 and m_3 denoting the shifting masses and r_1, r_2 and r_3 their shifting ranges along $\hat{i}$, $\hat{j}$ and $\hat{k}$ respectively.

As the controller has no information about the actual direction and magnitude of the aerodynamic force, an estimate $\hat{F}_{\text{aero}}$ needs to be used in the steering logic. A relative flow matching the inertial velocity and a mean atmospheric density are used to obtain this estimate.

The shifting masses position to achieve the requested perpendicular torque can be obtained using Eq. (46). Note that Eq. (46) is equivalent to the expression used to drive the magnetic torquers (replacing the magnetic field with the aerodynamic force $\hat{F}_{\text{aero}}$ and the magnetic moment with the mr product).

$$\begin{bmatrix} m_1 r_1 \\ m_2 r_2 \\ m_3 r_3 \end{bmatrix} = \frac{\tau_{req} \times \hat{F}_{\text{aero}} \left(M + m_1 + m_2 + m_3\right)}{\hat{F}_{\text{aero}} \cdot \hat{F}_{\text{aero}}} \tag{46}$$

It is clear from Eq. (45) that the shifting masses aerodynamic torque is perpendicular to the F_{aero} and thus other actuators should provide the required torque that is parallel to F_{aero}.

To reduce the complexity of the system only two shifting masses shifting along pitch $\hat{j}$ or yaw $\hat{k}$ will be used (thus $r_1 = 0$) and a single ideal actuator will be acting along the roll $\hat{i}$ axis. This configuration has been used to stabilize a 25 cm spacecraft with a random initial attitude and an initial angular velocity in a random orientation with a magnitude between $\pm 0.5\,\text{deg/s}$ (chosen with a random uniform distribution). Figure 7 shows the mean and the 3σ maximum stabilization time obtained by a 25 sample Monte Carlo simulation. The control law gains have been set according to Eq. (44) with a bandwidth of twice the spacecraft natural frequency and $\xi = 0.7$. The shifting masses represent 6% of the host vehicle mass (3% each shifting mass) and the CoM leads the CoP by 3% of the spacecraft radius.

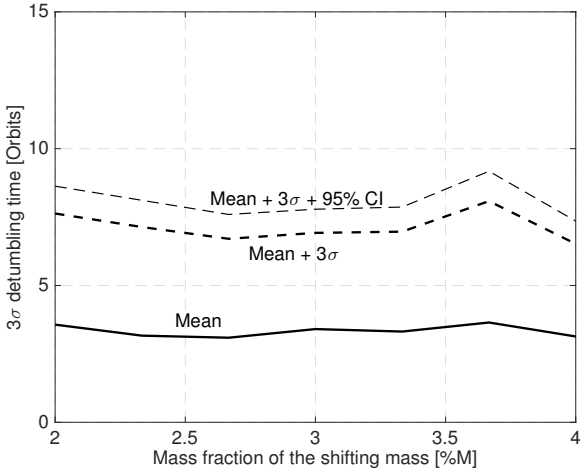

Figure 7. Stabilization Time.

PRACTICAL IMPLEMENTATION ON A 3U CUBESAT

Small spacecraft are more sensitive to aerodynamic disturbances due to their high area to inertia ratio. A CubeSat operating at low altitude is thus a good first candidate to implement the proposed aerodynamic disturbance rejection method.

A preliminary design of the "Shift-Mass Sat" 3U CubeSat with three orthogonal shifting masses is shown in Figure 8. All the components, subsystems and shifting masses, are COTS materials to ensure their commercial availability.

The three 150 g shifting masses approximately take 75% of the 1U volume and have a 70 mm useful shifting range. Magnetic torquers augment the shifting masses and complete the actuator set.

This design is then used for a simulation using a LQR control. The CoM position, mass, inertia, shifting mass and travel range, magnetic dipole moment of the magnetic torquers and aerodynamic properties are derived from the prototype design. For this particular design, the shifting masses have a 1.82 mm control authority on the vehicle's CoM position to modulate the aerodynamic torque direction and magnitude.

The LQR controller is used for detumbling and to keep the spacecraft stable. A gain schedule scheme, where less aggressive gains are employed during the detumbling phase. is employed. The

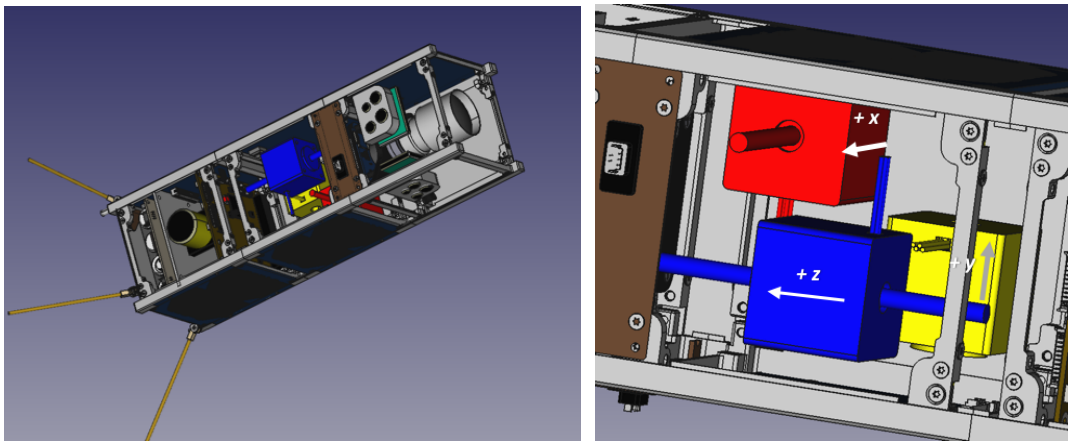

(a) (b)

Figure 8. Prototype 3U CubeSat Design (a) and Detail of the Three Orthogonal Shifting Masses (b).

initial angular velocity of the CubeSat is chosen as 0.01 rad/s in all axis and the orbit altitude is set at 300 km. The shifting masses movement and Euler angles of one of this simulation are presented in Figure 9.

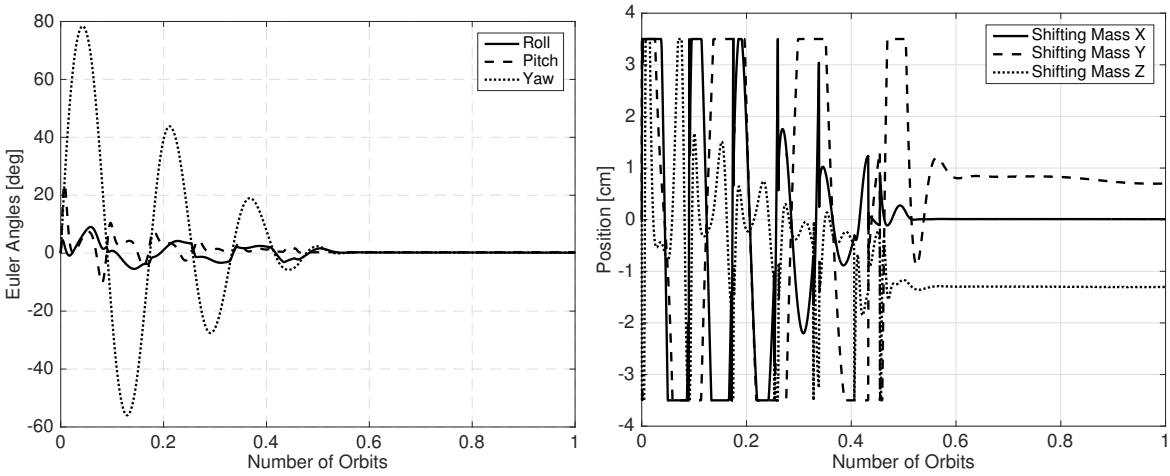

(a) (b)

Figure 9. Euler Angles (a) and Shifting Masses Positions (b).

It is also worth noting that the shifting masses exhibit a bias when the spacecraft is stabilized. This is because the CubeSat center of mass is not completely centered around the roll axis (as it was assumed on the previous sections).

CONCLUSION

Using a set of shifting masses is a viable method to reject the aerodynamic disturbances. Despite the highly non-linear dynamic of a spacecraft with internal moving parts simple controllers based on the linearized equations of motion suffice to keep the spacecraft stable with reasonable

requirements on the attitude determination subsystem and the shifting masses (shifting range and mass fraction). Achieving stabilization from arbitrary initial attitude and small angular velocities. A prototype implementation on a 3U CubeSat only using commercial-off-the-shelf components and a linear-quadratic-regulator controller demonstrates its technological feasibility. Other types of controllers, specially non-linear controllers, could be used to drive the shifting masses increasing the performance of the system.

REFERENCES

[1] J. Virgili Llop, P. C. Roberts, Z. Hao, L. R. Tomas, and V. Beauplet, "Very Low Earth Orbit mission concepts for Earth Observation. Benefits and challenges.," *Reinventing Space Conference, 18-21 November, London, UK*, Vol. BIS-RS-2014-37, 2014.

[2] J. Virgili Llop, *Spacecraft Flight in the Atmosphere*. PhD thesis, School of Engineering, Cranfield University, September 2014.

[3] A. Shao, E. A. Koltz, and J. R. Wertz, "Quantifying the Cost Reduction Potential for Earth Observation Satellites," *12th Reinventing Space Conference, 18-20 November 2014, London, UK*.

[4] J. Wertz, N. Sarzi-Amade, A. Shao, C. Taylor, and R. Van Allen, "Moderately Elliptical Very Low Orbits (MEVLOs) as a Long-Term Solution to Orbital Debris," *26th Annual AIAA/USU Conference on Small Satellites, Logan, UT*, Vol. SSC12-IV-6, 2012.

[5] J. Virgili Llop, P. C. E. Roberts, K. Palmer, S. Hobbs, and J. Kingston, "Descending Sun-Synchronous Orbits with Aerodynamic Inclination Correction," *Journal of Guidance, Control, and Dynamics*, Vol. 38, No. 5, 2014, pp. 831–842.

[6] J. Virgili, P. C. E. Roberts, and N. C. Hara, "Atmospheric Interface Reentry Point Targeting Using Aerodynamic Drag Control," *Journal of Guidance, Control, and Dynamics*, Vol. 38, No. 3, 2015, pp. 403–413.

[7] R. Bevilacqua and M. Romano, "Rendezvous Maneuvers of Multiple Spacecraft Using Differential Drag Under J2 Perturbation," *Journal of Guidance, Control, and Dynamics*, Vol. 31, 2014/06/09 2008, pp. 1595–1607.

[8] R. R. Kumar, D. D. Mazanek, and M. L. Heck, "Simulation and Shuttle Hitchhiker validation of passive satellite aerostabilization," *Journal of Spacecraft and Rockets*, Vol. 32, No. 5, 1995, pp. 806–811.

[9] R. R. Kumar, D. D. Mazanek, and M. L. Heck, "Parametric and classical resonance in passive satellite aerostabilization," *Journal of Spacecraft and Rockets*, Vol. 33, No. 2, 1996, pp. 228–234.

[10] M. L. Psiaki, "Nanosatellite Attitude Stabilization Using Passive Aerodynamics and Active Magnetic Torquing," *Journal of Guidance, Control, and Dynamics*, Vol. 27, No. 3, 2004, pp. 347–355.

[11] M. R. Drinkwater, R. Haagmans, D. Muzi, A. Popescu, R. Floberghagen, M. Kern, and M. Fehringer, "The GOCE Gravity Mission: ESA's First Core Earth Explorer," *Proceedings of the 3rd International GOCE User Workshop, 6-8 November, 2006, Frascati, Italy*, ESA, 2007, pp. 1–8.

[12] D. S. Bowman and M. J. Lewis, "Minimum Drag Power-Law Shapes for Rarefied Flow," *AIAA Journal*, 2002.

[13] K. Moe and M. M. Moe, "Gas-Surface Interactions in Low-Earth Orbit," *27th International Symposium on Rarefied Gas Dynamics, 2010*, American Institute of Physics, 10-15 July 2010, Pacific Grove, CA, USA 2010.

[14] D. M. Prieto, B. P. Graziano, and P. C. Roberts, "Spacecraft drag modelling," *Progress in Aerospace Sciences*, Vol. 64, 2014, pp. 56 – 65.

[15] M. F. Larsen and C. G. Fesen, "Accuracy issues of the existing thermospheric wind models: can we rely on them in seeking solutions to wind-driven problems?," *Annales Geophysicae*, Vol. 27, No. 6, 2009, pp. 2277–2284.

[16] C. Pardini, K. Moe, and L. Anselmo, "Thermospheric density model biases at the 23rd sunspot maximum," *Planetary and Space Science*, Vol. 67, No. 1, 2012, pp. 130 – 146.

[17] W. J. Larson and J. R. Wertz, *Space Mission Analysis and Design*. Space Technology Library, 3rd: Microcosm Press, 2005.

[18] P. W. Fortescue and J. P. W. Stark, *Spacecraft Systems Engineering, 4th Edition*. Wiley and Sons, Inc, 1995.

[19] T. L. Edwards and M. H. Kaplan, "Automatic Spacecraft Detumbling by Internal Mass Motion," *AIAA Journal*, Vol. 12, No. 4, 1974, pp. 496–502.

[20] B. Kunciw and M. Kaplan, "Optimal space station detumbling by internal mass motion," *Automatica*, Vol. 12, No. 5, 1976, pp. 417 – 425.

[21] H. Hamidi-Hashemi, "Liapunov analysis of a two dimensional unconstrained particle motion in a rigid body spinning about the thrust axis," *Circuits and Systems, 1993., Proceedings of the 36th Midwest Symposium on*, Aug 1993, pp. 971–973 vol.2.

[22] D. M. Halsmer and D. L. Mingori, "Nutational stability and passive control of spinning rockets with internal mass motion," *Journal of Guidance, Control, and Dynamics*, Vol. 18, No. 5, 1995, pp. 1197–1203.

[23] F. L. Janssens and J. C. v. d. Ha, "Stability of Spinning Satellite Under Axial Thrust, Internal Mass Motion, and Damping," *Journal of Guidance, Control, and Dynamics*, Vol. 38, No. 4, 2014, pp. 761–771.

[24] B. Wie, "Solar Sail Attitude Control and Dynamics, Part 1," *Journal of Guidance, Control, and Dynamics*, Vol. 27, No. 4, 2004, pp. 526–535.

[25] B. Wie and D. Murphy, "Solar-Sail Attitude Control Design for a Flight Validation Mission," *Journal of Spacecraft and Rockets*, Vol. 44, No. 4, 2007, pp. 809–821.

[26] C. Scholz, D. Romagnoli, B. Dachwald, and S. Theil, "Performance analysis of an attitude control system for solar sails using sliding masses," *Advances in Space Research*, Vol. 48, No. 11, 2011, pp. 1822 – 1835.

[27] B. M. Atkins and T. A. Henderson, "Under-Actuated Moving Mass Attitude Control for a 3U Cubesat Mission," *Advances in the Astronautical Sciences*, Vol. 143, 2012, pp. 2083 – 2094.

[28] K. Kumar, *Attitude Control of Miniature Satellites Using Movable Masses*. American Institute of Aeronautics and Astronautics, 2010.

[29] Y. T. Ahn, *Attitude Dynamics and Control of a Spacecraft Using Shifting Mass Distribution*. PhD thesis, The Pennsylvania State University, 2012.

[30] S. Chesi, *Attitude Control of NanoSatellite Using Shifting Masses*. PhD thesis, University of California, Santa Cruz, 2014.

[31] C. Grubin, "Dynamics of a Vehicle Containing Moving Parts," *Journal of Applied Mechanics*, Vol. 29, 09 1962, pp. 486–488.

[32] J. M. Picone, A. E. Hedin, D. P. Drob, and A. C. Aikin, "NRLMSISE-00 empirical model of the atmosphere: Statistical comparisons and scientific issues," *Journal of Geophysical Research: Space Physics*, Vol. 107, No. A12, 2002.

[33] ECSS Secretariat, "ECSS Space Engineering - Space Environment," Tech. Rep. ECSS-E-ST-10-04C, ESA, 2008.

[34] ISO 14222, "ISO 14222 Space environment (natural and artificial). Earth upper atmosphere," Tech. Rep. ISO 14222:2013, ISO, September 2013.

[35] R. Challinor, "The apparent rotation of the upper atmosphere," *Planetary and Space Science*, Vol. 16, No. 5, 1968, pp. 557–566.

[36] D. G. King-Hele, *Satellite Orbits in an Atmosphere: Theory And Application*. Blackie Academic and Professional, 1987.

[37] D. King-Hele, "The upper atmosphere as sensed by satellite orbits," *Planetary and Space Science*, Vol. 40, No. 2–3, 1992, pp. 223 – 233.

[38] D. King-Hele and D. M. Walker, "Upper-atmosphere zonal winds from satellite orbit analysis: An update," *Planetary and Space Science*, Vol. 36, No. 11, 1988, pp. 1085 – 1093.

[39] T. L. Killeen, P. B. Hays, N. W. Spencer, and L. E. Wharton, "Neutral winds in the polar thermosphere as measured from Dynamics Explorer," *Geophysical Research Letters*, Vol. 9, No. 9, 1982, pp. 957–960.

[40] A. E. Hedin, E. L. Fleming, A. H. Manson, F. J. Schmidlin, S. K. Avery, R. R. Clark, S. J. Franke, G. J. Fraser, T. Tsuda, F. Vial, and R. A. Vincent, "Empirical wind model for the middle and lower atmosphere.," *Journal of Atmospheric and Terrestrial Physics*, Vol. 58, No. 13, 1996, pp. 1421–1447.

[41] D. P. Drob, J. T. Emmert, G. Crowley, J. M. Picone, G. G. Shepherd, W. Skinner, P. Hays, R. J. Niciejewski, M. Larsen, C. Y. She, J. W. Meriwether, G. Hernandez, M. J. Jarvis, D. P. Sipler, C. A. Tepley, M. S. O'Brien, J. R. Bowman, Q. Wu, Y. Murayama, S. Kawamura, I. M. Reid, and R. A. V. and, "An empirical model of the Earth's horizontal wind fields: HWM07," *Journal of Geophysical Research: Space Physics*, Vol. 113, No. A12304, 2008.

[42] G. A. Bird, *Molecular Gas Dynamics and the Direct Simulation of Gas Flows*. Oxford Science Publications, 1994.

[43] L. Sentman, *Free Molecule Flow Theory and Its Application to the Determination of Aerodynamic Forces*. Lockheed Missile and Space Co., 1961.

[44] K. Moe and M. M. Moe, "Gas-surface interactions and satellite drag coefficients," *Planetary and Space Science*, Vol. 53, No. 8, 2005, pp. 793–801.

[45] J. C. Gregory and P. N. Peters, "A measurement of the angular distribution of 5 eV atomic oxygen scattered off a solid surface in Earth orbit," *Proceedings of the 15th international symposium on rarefied gas dynamics* (V. Boffi and C. Cercignani, eds.), Vol. 1, 1987, pp. 644–656.

[46] K. Moe, M. M. Moe, and S. D, "Improved satellite drag coefficient calculations from orbital measurements of energy accommodation," *Journal of Spacecraft and Rockets*, Vol. 35, No. 3, 1998, pp. 266–272.

[47] E. K. Sutton, "Normalized Force Coefficients for Satellites with Elongated Shapes," *Journal of Spacecraft and Rockets*, Vol. 46, 2013/12/13 2009, pp. 112–116.

[48] G. Koppenwallner, "Energy accommodation coefficient and momentum transfer modeling," HTG–TN–08–11, HTG, Katlenburg Lindau, 2009.

[49] E. Doornbos, *Thermospheric Density and Wind Determination from Satellite Dynamics*. PhD thesis, Technische Universiteit Delft, 2011.

[50] B. Wie and P. M. Barba, "Quaternion feedback for spacecraft large angle maneuvers," *Journal of Guidance, Control, and Dynamics*, Vol. 8, No. 3, 1985, pp. 360–365.

[51] B. Wie, H. Weiss, and A. Arapostathis, "Quarternion feedback regulator for spacecraft eigenaxis rotations," *Journal of Guidance, Control, and Dynamics*, Vol. 12, No. 3, 1989, pp. 375–380.